Crabtree and Morris.[20,21] The relative effectiveness of the rhodium and iridium catalysts and a comparison with the reactivity of Wilkinson's catalyst, $[RhCl(PPh_3)_3]$, in these reactions[22] might be related to the ability of the metal ions to polarize the ligand differently in the two oxidation states.

Acknowledgment. We thank Dr. John Petersen of Clemson University for the gift of $[Rh(NH_3)_5py](ClO_4)_3$. We gratefully acknowledge support of this project by the PSC-BHE grant program of the City University of New York.

Registry No. $[Co(NH_3)_5py]^{3+}$, 31011-67-3; $[Rh(NH_3)_5py]^{3+}$, 60118-45-8; $[Zh(H_2O)_5py]^{2+}$, 45985-08-8; $[Cd(H_2O)_5py]^{2+}$, 20154-57-8; $[Ag(H_2O)_5py]^{+}$, 78370-96-4.

(20) Crabtree, R. H. *J. Organomet. Chem.* **1977**, *141*, 113–121.
(21) Crabtree, R. H.; Morris, G. E. *J. Organomet. Chem.* **1977**, *141*, 205–215.
(22) Crabtree, R. H. *Acc. Chem. Res.* **1979**, *12*, 331–337.

Contribution from the Departments of Chemistry, University of Denver, Denver, Colorado 80208, and University of Colorado at Denver, Denver, Colorado 80202

Metal–Nitroxyl Interactions. 21. Conformational Effects on Spin–Spin Interaction in Three Spin-Labeled Copper Porphyrins

BHIMRAO M. SAWANT, GARY A. BRADEN, ROBERT E. SMITH, GARETH R. EATON,* and SANDRA S. EATON

Received November 13, 1980

Electron–electron spin–spin interaction has been observed in the room-temperature solution EPR spectra of three spin-labeled copper porphyrins. For a piperidine nitroxyl attached to a porphyrin pyrrole position, the electron–electron coupling constant, J, was greater for an ester linkage than for an amide linkage which correlates with greater porphyrin–side-chain conjugation in the ester derivative than in the amide derivative. The larger temperature dependence of J for the ester derivative than for the amide derivative is consistent with the greater flexibility of ester linkages than of amide linkages. When a pyrrolidine nitroxyl was attached to the porphyrin by an amide linkage, J was strongly temperature dependent which was attributed to conformational mobility of the pyrrolidine ring or of the amide–nitroxyl ring linkage.

Introduction

The widespread use of nitroxyl radicals as spin labels in biological systems has led to increased interest in the nature of spin–spin interactions between nitroxyls and transition-metal ions.[1] To increase our understanding of the factors which influence the exchange component of spin–spin interactions, we have prepared the spin-labeled porphyrins I–III, obtained

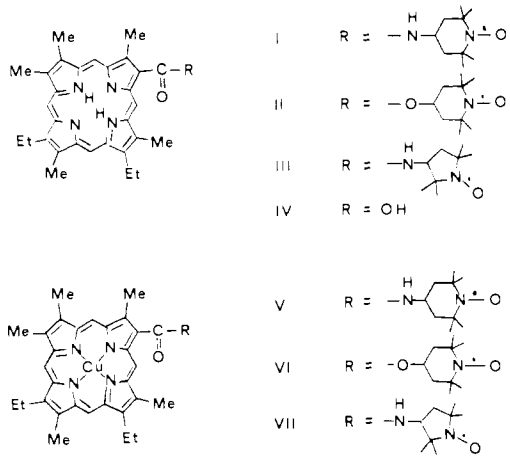

from IV,[2] and the corresponding copper complexes V–VII. Porphyrin IV was chosen for study because of its similarity to naturally occurring porphyrins, the possibility of inserting a variety of metal ions, and the presence of a single reactive side chain for attachment of a nitroxyl group. In the initial studies with this porphyrin, copper complexes V–VII were prepared in order to assess the effect of ester and amide linkages and of five- and six-membered nitroxyl rings on spin–spin-exchange interactions. Some preliminary EPR studies of V have been reported.[3]

Table I. Electron-Electron Coupling Constants at Room Temperature[a]

complex	solvent	J, G	10^4J, cm^{-1}
V	$CHCl_3$	78[b,c]	74
V	C_2HCl_3	81[b,c]	77
V	CH_2Cl_2	82[b,c]	78
V	ethyl acetate	82[b]	78
V	toluene	83[b]	79
V	$CHBr_3$	84[b]	80
V	benzene	85[b]	81
V	Me_2SO	87[b]	83
V	DMF	88[b]	84
V	pyridine	90[b]	86
V	CS_2	92[b]	88
VI	$CHCl_3$	210[c,d]	201
VI	$CHBr_3$	215[d]	206
VI	CH_2Cl_2	220[c,d]	210
VI	C_2HCl_3	220[d]	210
VI	1:1 toluene/THF	220[d]	210
VI	pyridine	220[d]	210
VII	$CHCl_3$	~100[c]	~96
VII	CH_2Cl_2	~100[c,e]	~96
VII	C_2HCl_3	~100[e]	~96
VII	pyridine	~100[e]	~96

[a] Values of J based on computer simulation of X-band EPR spectra unless otherwise noted. [b] Uncertainty ±1 G. [c] Spectra simulated at both X band and Q band. [d] Uncertainty ±5 G. [e] Uncertainty ±15 G.

Experimental Section

Infrared spectra were obtained in Nujol mulls on a Perkin-Elmer 337 grating spectrometer. Electronic spectra were obtained in

* To whom correspondence should be addressed at the University of Denver.

(1) Eaton, G. R.; Eaton, S. S. *Coord. Chem. Rev.* **1978**, *26*, 207–262.
(2) Schwartz, F. P.; Gouterman, M.; Muljiani, Z.; Dolphin, D. *Bioinorg. Chem.* **1972**, *2*, 1–32.
(3) Braden, G. A.; Trevor, K. T.; Neri, J. M.; Eaton, G. R.; Eaton, S. S. *J. Am. Chem. Soc.* **1977**, *99*, 4854–4855.

0020-1669/81/1320-3349$01.25/0

chloroform solution on a Beckman Acta V spectrometer. Data are given below with wavelengths in nanometers and log ϵ in parentheses. X-Band EPR spectra were obtained on a Varian E-9 spectrometer as previously described.[4] Q-Band EPR spectra were obtained with the use of a Harvey-Wells magnet and a Varian microwave bridge interfaced to the E-9 console and Varian 620L computer.[5] EPR spectra in the figures are shown with magnetic field increasing to the right. *g*-Values were measured relative to DPPH (2.0036). EPR spectra were run on degassed samples with concentrations about 10^{-3} M. Values of the electron–electron coupling constant, *J*, are given in both gauss and reciprocal centimeters in Table I. However, so that discussion of the field-swept experimental spectra can be facilitated, *J* is given in gauss throughout the following text (1.0 G = 0.1 mT). EPR and electronic spectra were obtained in dry purified solvents.

Preparation of Compounds. 2-Carboxy-12,17-diethyl-3,7,8,13,18-pentamethylporphyrin (IV) was prepared by the method of Dolphin et al.[2] Pyrrole precursors were made by literature methods: 2,3,4-trimethylpyrrole,[6] diethyl 2,4-dimethylpyrrole-3,5-dicarboxylate,[7] *tert*-butyl 4-ethyl-3,5-dimethylpyrrole-2-carboxylate,[8] and 5-bromo-5′-bromomethyl-3,4′-diethyl-3′,4-dimethylpyrromethane hydrobromide.[9] In our hands the reported yield of 5-bromo-5′-bromomethyl-3,4′-diethyl-3′,4-dimethylpyrromethane hydrobromide[9] could only be obtained when the reaction was run in a nitrogen atmosphere with minimum lighting and with the use of ether which had been freshly distilled from $LiAlH_4$.

Spin-Labeled Porphyrins. 2-(((2,2,6,6-Tetramethyl-1-oxypiperidine-4-yl)amino)carbonyl)-7,12-diethyl-3,8,13,17,18-pentamethylporphyrin (I). A mixture of the porphyrin acid IV (150 mg, 3.1×10^{-4} moles) and freshly distilled thionyl chloride (5 mL) was heated in a nitrogen atmosphere at 50–60 °C for 3–4 h. After the mixture was cooled, 15 mL of dry benzene was added. Benzene and unreacted thionyl chloride were removed in vacuo. The resulting acid chloride was dried in vacuo at ~60 °C for 2 h. The solid was dissolved in 75 mL of dry THF and 2 mL of pyridine. The solution was heated to reflux, and 200 mg of 4-amino-2,2,6,6-tetramethylpiperidinyl-1-oxy was added. The solution was refluxed overnight. After the solvent was removed in vacuo, the residue was dissolved in $CHCl_3$ and washed with saturated aqueous sodium acetate and then with water. The $CHCl_3$ solution was dried over Na_2SO_4, and the solvent was removed in vacuo. The product was dissolved in $CHCl_3$ and chromatographed on silica gel. The second band (deep red) eluted with $CHCl_3$ was collected. The product was recrystallized from CH_2Cl_2/heptane; yield 50%. IR: ν_{NH} 3420, ν_{CO} 1610 cm^{-1}. VIS ($CHCl_3$) (log ϵ): 623 (3.11), 568 (3.77), 542 (4.11), 505 (4.00), 405 (5.22). EPR ($CHCl_3$): g = 2.0059, A_N = 15.8 G. Anal. Calcd for $C_{39}H_{49}N_6O_2$: C, 73.90; H, 7.79; N, 13.26. Anal. Calcd for $C_{39}H_{49}N_6O_2 \cdot 0.69CH_2Cl_2$: C, 69.45; H, 7.39; N, 12.27; Cl, 6.21. Found: C, 69.45; H, 7.32; N, 12.37; Cl, 6.29.

2-(((2,2,6,6-Tetramethyl-1-oxypiperidin-4-yl)oxy)carbonyl)-7,12-diethyl-3,8,13,17,18-pentamethylporphyrin (II). The ester was prepared from the acid chloride of porphyrin IV and 4-hydroxy-2,2,6,6-tetramethylpiperidinyl-1-oxy as described above for I; yield 48%. IV: ν_{NH} 3420, ν_{CO} 1680 cm^{-1}. VIS ($CHCl_3$) (log ϵ): 633 (3.06), 574 (3.93), 550 (4.20), 510 (3.98), 407 (5.26). EPR ($CHCl_3$): g = 2.0059, A_N = 15.8 G. Anal. Calcd for $C_{39}H_{48}N_5O_3$: C, 73.79; H, 7.62; N, 11.03. Found: C, 73.50; H, 7.51; N, 10.91.

2-(((2,2,5,5-Tetramethyl-1-oxypyrrolidin-3-yl)amino)carbonyl)-7,12-diethyl-3,8,13,17,18-pentamethylporphyrin (III). The amide was prepared from the acid chloride of porphyrin IV and 3-amino-2,2,5,5-tetramethylpyrrolidinyl-1-oxy as described above for I; yield 41%. IR: ν_{NH} 3400, ν_{CO} 1620 cm^{-1}. VIS ($CHCl_3$) (log ϵ): 624 (3.18), 568 (3.86), 543 (4.09), 508 (3.98), 402 (5.24). EPR ($CHCl_3$): g = 2.0059, A_N = 14.8 G. Anal. Calcd for $C_{38}H_{47}N_6O_2$: C, 73.64; H, 7.64; N, 13.56. Found: C, 73.44; H, 7.47; N, 13.16.

Copper Complexes. Copper(II) 2-(((2,2,6,6-Tetramethyl-1-oxypiperidin-4-yl)amino)carbonyl)-7,12-diethyl-3,8,13,17-pentamethylporphyrin (V). To a refluxing solution of 50 mg of I (7.9×10^{-5} mol) in 50 mL of $CHCl_3$ was added 50 mg (2.5×10^{-4} mol) of cupric acetate hydrate in 15 mL of hot methanol. The solution was refluxed for 10 min. The visible spectrum indicated complete conversion to the copper complex. The solvent was removed on a rotary evaporator. The solid was dissolved in $CHCl_3$, and the solution was washed with water. After the solution was dried over Na_2SO_4, the volume was reduced to a few milliliters and placed on a silica gel column. The column was eluted with $CHCl_3$. The second band (red) was collected. The solvent was removed, and the product was recrystallized from $CHCl_3$/heptane; yield 54%. IR: ν_{NH} 3350, ν_{CO} 1620 cm^{-1}. VIS ($CHCl_3$) (log ϵ): 573 (4.38), 533 (4.22), 403 (5.53). VIS (pyridine) (log ϵ): 573 (4.42), 537 (4.38), 410 (5.52). Anal. Calcd for $C_{39}H_{47}N_6O_2Cu \cdot 0.18CHCl_3$: C, 65.68; H, 6.64; N, 11.73; Cl, 2.62. Found: C, 65.71; H, 6.83; N, 11.62; Cl, 2.78.

Copper(II) (((2,2,6,6-Tetramethyl-1-oxypiperidin-4-yl)oxy)carbonyl)-7,12-diethyl-3,8,13,17,18-pentamethylporphyrin (VI). The copper complex was prepared from porphyrin II and cupric acetate as described above for V. The product was recrystallized from CH_2Cl_2/heptane; yield 65%. IR: ν_{CO} 1710 cm^{-1}. VIS ($CHCl_3$) (log ϵ): 584 (4.42), 542 (4.12), 412 (5.41). VIS (pyridine) (log ϵ): 586 (4.24), 548 (4.05), 419 (5.19). Anal. Calcd for $C_{39}H_{46}N_5O_3Cu$: C, 67.27; H, 6.66; N, 10.06. Anal. Calcd for $C_{39}H_{46}N_5O_3Cu \cdot 0.39CH_2Cl_2$: C, 64.86; H, 6.46; N, 9.60; Cl, 3.78. Found: C, 64.94; H, 6.39; N, 9.36; Cl, 3.84.

Copper(II) 2-(((2,2,5,5-Tetramethyl-1-oxypyrrolidin-3-yl)amino)carbonyl)-7,12-diethyl-3,8,13,17,18-pentamethylporphyrin (VII). The copper complex was prepared from porphyrin III and cupric acetate as described above for V and recrystallized from CH_2Cl_2/heptane; yield 42%. IR: ν_{NH} 3360, ν_{CO} 1620 cm^{-1}. VIS ($CHCl_3$) (log ϵ): 574 (4.31), 534 (4.11), 402 (5.45). VIS (pyridine) (log ϵ): 572 (4.20), 535 (4.11), 403 (5.28). In pyridine solution, each band had a shoulder on the low-energy side, consistent with the presence of both VII and VII·(pyridine). Anal. Calcd for $C_{38}H_{45}N_6O_2Cu$: C, 66.99; H, 6.66;, N, 12.33. Anal. Calcd for $C_{38}H_{45}N_6O_2Cu \cdot 0.20CH_2Cl_2$: C, 65.67; H, 6.55; N, 12.03; Cl, 2.08. Found: C, 65.88; H, 6.60; N, 12.19; Cl, 2.35.

Computer Simulations

The EPR spectra were simulated with the use of the computer program CUNO which is based on the Hamiltonian[10] given in eq 1, where g_1 and g_2 are the g values of the metal

$$\mathcal{H} = g_1\beta H\hat{S}_{1Z} + g_2\beta H\hat{S}_{2Z} + hJ\hat{S}_{1Z}\hat{S}_{2Z} + (hJ/2)(\hat{S}_{1+}\hat{S}_{2-} + \hat{S}_{1-}\hat{S}_{2+}) + hA_M\hat{S}_{1Z}\hat{I}_{1Z} + hA_N\hat{S}_{1Z}\hat{I}_{2Z} + hA_{N'}\hat{S}_{2Z}\hat{I}_{3Z} + (hA_M/2)(\hat{S}_{1+}\hat{I}_{1-} + \hat{S}_{1-}\hat{I}_{1+}) - g_M\beta_N H\hat{I}_{1Z} - g_N\beta_N H\hat{I}_{2Z} - g_{N'}\beta_N H\hat{I}_{3Z} \quad (1)$$

and nitroxyl electrons, $\hat{S}_1$ and $\hat{S}_2$ refer to the metal and nitroxyl electron spins, respectively, J is the electron–electron coupling constant in hertz, I_1, I_2, and I_3 refer to the metal electron spin, the nuclear spin of the coordinated nitrogens, and the nuclear spin of the nitroxyl nitrogen, respectively, A_M is the metal electron–metal nuclear coupling constant in hertz, A_N is the coupling constant in hertz between the metal electron and the nuclear spins of the coordinated nitrogens, $A_{N'}$ is the coupling constant in hertz between the nitroxyl electron and the nuclear spin of the nitroxyl nitrogen, and all other symbols are defined as in ref 10. The first seven terms in the Hamiltonian were treated exactly, and the last four were treated as a peturbation to second order for the transition energies and to first order for the transition probabilities. So that visual comparison with the field-swept experimental spectra could be facilitated, the values of J, A_M, A_N, and $A_{N'}$ are discussed below in units of gauss with the conversion between hertz and gauss given by eq 2–4. The conversion factor for A_N is the same as for A_M. Only the absolute value of J can be determined from these experiments.

(4) More, K. M.; Eaton, G. R.; Eaton, S. S. *Inorg. Chem.* **1979**, *18*, 2492–2496.
(5) Eaton, S. S.; More, K. M.; DuBois, D. L.; Boymel, P. M.; Eaton, G. R. *J. Magn. Reson.* **1980**, *41*, 150–157.
(6) Clezy, P. S.; Nichol, A. W. *Aust. J. Chem.* **1965**, *18*, 1835–1845.
(7) "Organic Syntheses"; Wiley: New York; Collect. Vol. II, pp 202–204.
(8) Johnson, A. W.; Kay, I. T.; Markham, E.; Price, R.; Shaw, K. B. *J. Chem. Soc.* **1959**, 3416–3424.
(9) Smith, K. M. *J. Chem. Soc., Perkin Trans. 1* **1972**, 1471–1475.
(10) Eaton, S. S.; DuBois, D. L.; Eaton, G. R. *J. Magn. Reson.* **1978**, *32*, 251–263.

$$J\,(\mathrm{G}) = [J\,(\mathrm{Hz})]\frac{h}{2\beta}\left(\frac{1}{g_1} + \frac{1}{g_2}\right) \quad (2)$$

$$A_{\mathrm{M}}\,(\mathrm{G}) = [A_{\mathrm{M}}\,(\mathrm{Hz})]\frac{h}{g_1\beta} \quad (3)$$

$$A_{\mathrm{N}'} = [A_{\mathrm{N}'}\,(\mathrm{Hz})]\frac{h}{g_2\beta} \quad (4)$$

The electron–electron coupling results in AB quartet patterns in the EPR spectra. The lines in the spectra are referred to as copper or nitroxyl depending on the nature of the transitions as J approaches 0. When J is small relative to the g-value difference between the copper and nitroxyl electrons, each of the copper and nitroxyl lines is split into a doublet. As J becomes larger, the intensity of the outer lines of the AB pattern goes to 0 and the positions of the inner copper and inner nitroxyl lines become equal.

In the EPR spectra of the spin-labeled copper porphyrins V and VI, the outer nitroxyl lines were observed and the value of J was determined from the splitting between the inner and outer nitroxyl lines. The outer lines were not detected in the EPR spectra of VII so the value of J is based on the shape of the inner lines which are partially overlapping. The overall line shape is also dependent on the assumed line widths so the values of J for VII are less certain than those for V and VI. The copper regions of the EPR spectra of VI and VII are poorly resolved so the g and A values for the copper complex of the ethyl ester of porphyrin IV were used in the simulations (g = 2.0944, A_{Cu} = 86.0 G, A_{N} = 16.0 G in $CHCl_3$ solution and g = 2.0994, A_{Cu} = 82.0 G, and A_{N} = 15.5 G in pyridine solution). The spectra were consistent with these parameters within the uncertainty caused by the broad lines.

Results and Discussion

The spin-labeled porphyrins I–III were prepared from the acid chloride of porphyrin IV and the appropriate nitroxyl alcohol or amine. Porphyrin IV and its acid chloride are not stable to prolonged heating and high temperatures. Decomposition resulted in loss of the carbonyl stretch in the IR spectra. In some cases the characteristic porphyrin π–π^* electronic transitions also disappeared. Therefore reaction temperatures were carefully controlled. Minimum heating was also used in preparing the copper complexes. The limited solubilities of the products made chlorinated solvents necessary for recrystallization. However, the elemental analyses indicated that even after drying in vacuo for 2–3 weeks at 95 °C, chlorinated solvent was retained in the crystal lattice for some of the compounds. Interaction with H_2O was also observed in the EPR spectra of the copper complexes V and VI. Other specific interactions which were not characterized in this study may also contribute to the poor elemental analyses.

Electronic Spectra. The electronic spectra of the spin-labeled copper porphyrin amides V and VII in $CHCl_3$ and CH_2Cl_2 solution had bands at 572–574, 531–534, and 401–403 nm. However, for the spin-labeled copper porphyrin ester VI, the bands occurred at 584, 540–542, and 410–412 nm. The lower transition energies for the porphyrin π–π^* transitions of the ester than of the amides indicate that conjugation between the porphyrin π system and the substituent is greater for the ester than for the amides. Examination of space-filling molecular models indicates that steric interference between the amide N–H proton and the meso proton or ring methyl group prevents the amide groups from becoming coplanar with the porphyrin ring but the ester can be nearly coplanar. Thus steric effects appear to be responsible for the differences in the extent of conjugation. The bands in the visible spectra of the copper complexes V–VII in pyridine solution occur at lower energies than in $CHCl_3$ solution which indicates that pyridine coordinates to the copper porphyrins and causes changes in the energies of the porphyrin π orbitals.

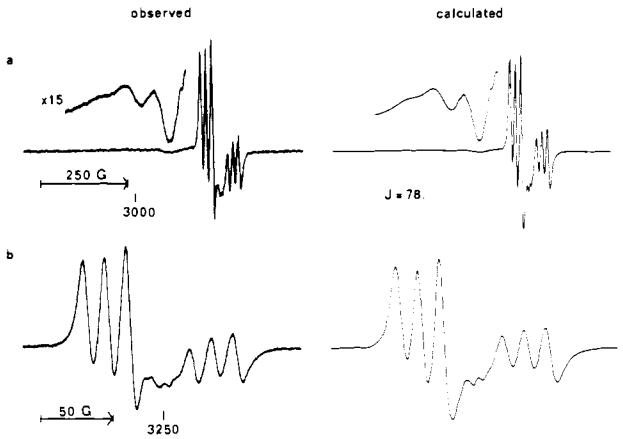

Figure 1. X-Band (9.11-GHz) EPR spectra of the spin-labeled copper porphyrin V in $CHCl_3$ solution at room temperature. (a) 800 G scan of the copper and nitroxyl signals obtained with 0.8 G modulation amplitude and 20 mW microwave power. Insert was obtained with product of modulation amplitude, gain, and square root of microwave power 15 times greater than for full spectrum. (b) 200 G scan of the nitroxyl signals obtained with 0.63 G modulation amplitude and 20 mW microwave power. The value of the electron–electron coupling constant, J, is given in gauss.

EPR Spectra. The X-band EPR spectra of the spin-labeled copper porphyrin amide V in $CHCl_3$ solution are shown in Figure 1. The nitroxyl signal is a doublet of triplets with a splitting of 78 G, which is superimposed on the high-field side of the copper lines. The copper lines are a doublet of quartets. Since J (78 G) is about the same size as A_{Cu} (86 G), the two copper quartets overlap to give a five-line pattern with the highest field line largely superimposed on the nitroxyl lines. At Q-band, the copper and nitroxyl lines are well separated but the copper signal is a single very broad line with no resolved hyperfine structure due to incomplete motional averaging of g and A anisotropy. When the Q-band spectra were run in solvents which had not been thoroughly dried, the nitroxyl region of the spectrum showed a broad line superimposed on the doublet of triplets. After the sample was shaken with water, the amplitude of the broad signal increased relative to that of the triplets. The spectra could be simulated by assuming a mixture of components with J = 78 G and $J \approx 0$ G. When solid samples of V which had been exposed to atmospheric moisture were used to obtain solution EPR spectra in dry solvents, components with J = 78 G and $J \approx 0$ G were observed. After the same solid sample had been dried in vacuo overnight, the EPR spectra in the same solvents showed only the presence of the component with J = 78 G. Apparently there is a reversible interaction between V and H_2O, and the lifetime of the V·H_2O complex is sufficiently long on the EPR time scale to permit observation of separate signals for V and V·H_2O. Since the value of J in pyridine solution is 90 G and the visible spectra indicate that pyridine coordinates to the copper in V, it appears that coordination of a ligand to copper does not cause a major change in J. Therefore it seems unlikely that the influence of water is via coordination to the copper. If the water were interacting with the amide or ester groups thereby changing the conformation of the linkage and changing the porphyrin to side chain conjugation, this would be expected to cause shifts in the bands in the visible spectra. The equilibrium constant is small enough that only about half of the complex exists as the water adduct in solutions which are $\sim \times 10^{-4}$ M in copper porphyrin. Thus the absence of observable shifts in the visible spectra cannot rule out the possibility of interaction with the ester or amide linkage. The interaction may be too weak to influence the IR spectra. If the water were hydrogen bonded to the nitroxyl group, the

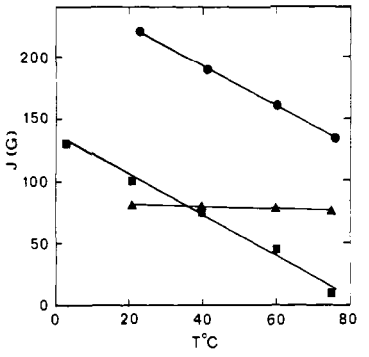

Figure 2. Plots of the temperature dependence of J in trichloroethylene solution for V (▲), VI (●), and VII (■).

change in spin density might be sufficient to cause the value of J to decrease. In this case a decrease in the nitroxyl A_N would also be expected. However, the line widths in the water adduct are too large to permit a determination of A_N. If the water is interacting with the nitroxyl group, it is suprising that the interaction is so much stronger for V and VI (see below) than for other spin-labeled copper complexes. Thus the available data do not permit assignment of the site of the water interaction. In another case we have previously observed the formation of a copper porphyrin–nitroxyl–halocarbon complex.[11] When V is dissolved in dry $CHCl_3$ or $CHBr_3$, there is no evidence of a second component in the EPR spectra.

As summarized in Table I, values of J were obtained for V in a variety of solvents. The values do not correlate with any single solvent parameter. The values of J in all of the chlorinated solvents fall on the small end of the range of observed values. This may be due to a weak nitroxyl-chlorinated solvent interaction and rapid exchange on the EPR time scale between free and coordinated nitroxyl. The variations in J may also reflect small conformational changes as a result of differences in solvation of both the porphyrin ring and the amide linkage. Values of J in C_2HCl_3 solution decreased slightly when the temperature was increased from 22 to 75 °C as shown in Figure 2. The nitroxyl line widths increased by about 1 G over this temperature interval.

The EPR spectrum of the spin-labeled copper porphyrin ester VI in dry $CHCl_3$ is shown in Figure 3a. The nitroxyl outer line occurs at 3410 G. Since Pyrex tubes frequently have a background signal in this region, all spectra of this compound were taken in quartz tubes to permit accurate determination of the line shape and position of the outer line. The position of this line requires a value of J of 210 G. The inner nitroxyl lines occur between 3100 and 3300 G. The copper lines are broad and poorly resolved. All of the lines in the spectrum are substantially broader than the lines in the spectra of the closely related amide, V. We have previously noted that increased line widths are usually observed when the value of J is uncertain due to molecular motion which interconverts conformations with different values of J.[11] The computer calculation truncates the contribution from a Lorentzian line at six line widths out from the center of the line. Thus the calculation shows the outer nitroxyl line on an essentially flat base line, whereas the experimental spectrum has a sloping base line due to the contribution from the broad inner lines. When a solid sample of VI was exposed to atmospheric moisture or when the dry solid was dissolved in solvents which had not been carefully dried, the spectrum shown in Figure 3b was obtained. When a solid sample of VI that had been exposed to moisture was subsequently dried in vacuo and used to obtain a solution EPR spectrum, the signal reverted to that in Figure 3a. Thus the change in the EPR spectrum can be

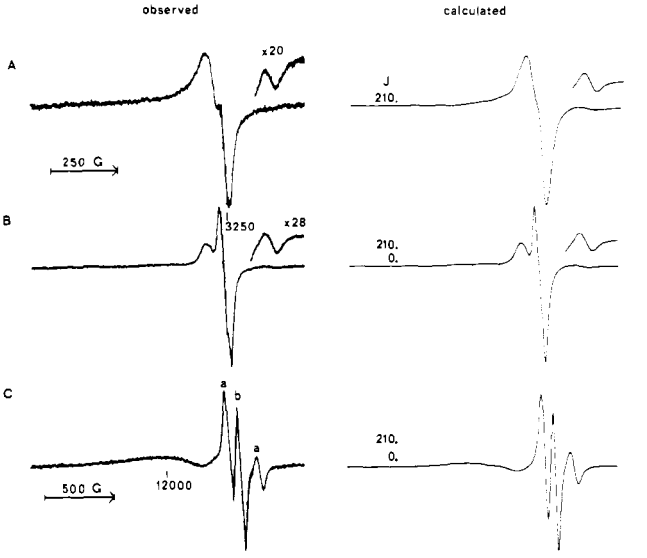

Figure 3. EPR spectra of the spin-labeled copper porphyrin VI in $CHCl_3$ solution at room temperature. (a) X-Band (9.11-GHz) spectrum of a freshly dried sample of VI in dry $CHCl_3$ obtained with 1000 G scan width, 1.0 G modulation amplitude, and 80 mW microwave power. Insert was obtained with product of modulation amplitude, gain, and square root of microwave power 20 times greater than for full spectrum. (b) X-Band (9.11-GHz) spectrum of a sample of VI which had been exposed to atmospheric moisture and then dissolved in dry $CHCl_3$ obtained with 1000 G scan width, 1.0 G modulation amplitude, and 20 mW microwave power. Insert was obtained with the product of modulation amplitude, gain, and square root of microwave power 28 times that for full spectrum. (c) Q-Band (35.25-GHz) spectrum of same sample as used for b. Spectrum was obtained with the use of 2000 G scan width, 1.0 G modulation amplitude, and 200 mW microwave power. J is given in gauss.

reversed by drying the solid sample. The solubility of VI in $CHCl_3$ is also increased by the presence of H_2O. In Figure 3b the intensity between 3210 and 3260 G is much greater than it is in Figure 3a. This difference is consistent with the presence of a component with $J \approx 0$. The computer simulation shown in Figure 3b was obtained assuming a 1:1 mixture of components with $J = 210$ and $J = 0$ G, respectively. The presence of two components in solution in the presence of H_2O is confirmed by the Q-band spectrum which is shown in Figure 3c. The nitroxyl region of the Q-band spectrum shows a doublet of lines (marked a in Figure 3c) due to a species with $J = 210$ G and a singlet (marked b) due to a species with $J \approx 0$ G. The nitroxyl line widths are sufficiently broad that the nitrogen hyperfine is not resolved. Since the visible spectra indicate that pyridine coordinates to the copper in VI and the value of J for VI in pyridine solution (220 G) is slightly larger than that in $CHCl_3$ solution, it seems unlikely that coordination of water to the copper could cause the observed decrease in J. However, as discussed above for V, the data do not permit assignment of the site of H_2O interaction. In $CHCl_3$ and $CHBr_3$ solution there is no evidence of a second component due to formation of a halocarbon adduct.

The low solubility of ester VI in most organic solvents precluded an extensive study of the solvent dependence of J. However, from the limited data available, it appears that J is not strongly solvent dependent at room temperature. In C_2HCl_3 solution, the value of J decreases sharply from 220 G at 23 °C to 135 G at 76 °C (Figure 2). The line widths increased as the temperature increased, and at high temperatures the outer nitroxyl lines were so broad that the signal was difficult to detect. The large temperature dependence of J and the line widths for the ester VI are in marked contrast with the slight temperature dependence of J and the line widths for amide V. Since the two compounds differ only in the

(11) More, K. M.; Eaton, S. S.; Eaton, G. R. *Inorg. Chem.* **1981**, *20*, 2641.

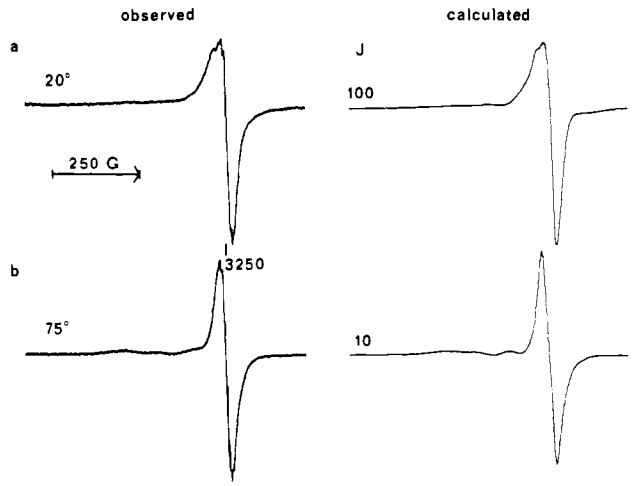

Figure 4. X-Band (9.11-GHz) EPR spectra of the spin-labeled copper porphyrin VII in trichloroethylene solution. The spectra are 1000 G scans obtained with 1.25 G modulation amplitude and 60 mW microwave power: (a) 20 °C; (b) 75 °C.

porphyrin–nitroxyl linkage, the differences in temperature dependence must be due to that linkage. The more flexible ester linkage permits a greater range of molecular motions than does the more rigid amide linkage. The increased motion of the ester linkage at higher temperatures could result in population of a variety of conformations which are less favorable for spin–spin interaction than those which are populated at room temperature. It is proposed that the greater range in values of J at high temperature and intermediate rates of averaging between forms with different values of J result in the observed line broadening at high temperature.

The EPR spectra of the spin-labeled copper porphyrin amide VII in C_2HCl_3 at 22 and 75 °C are shown in Figure 4. Even at higher microwave powers and modulation amplitudes no outer lines could be detected. The inability to detect outer lines could indicate that the value of J was large or that the outer lines were severely broadened. The intensity distribution of the observed lines indicates that a large fraction of the total intensity occurs between 3150 and 3275 G at room temperature. The nitroxyl lines represent half of the intensity of the EPR signal. When J is small, the nitroxyl inner and outer lines all occur within a narrow range near 3240 G (when ν is about 9.11 GHz as in these experiments). When J is small, the copper lines in the spectra of the spin-labeled copper porphyrins are much broader than the nitroxyl lines so the nitroxyl lines dominate the spectra. As the value of J increases, the intensity of the outer lines becomes negligible, the positions of the nitroxyl and copper lines approach each other, and the line widths of the copper and nitroxyl lines become similar. The spectrum approaches a four-line pattern with an apparent hyperfine splitting of 0.5 A_{Cu}. The spectrum in Figure 4a is characteristic of the case where J is small and the nitroxyl lines dominate the spectrum. The simulated spectrum in Figure 4a was obtained with J = 100 G. Similar agreement between observed and calculated spectra was obtained for J = 90–100 G. The line widths for the inner nitroxyl lines in the simulated spectrum range from 8 to 54 G, depending on the nuclear spin of the copper to which the nitroxyl is coupled. The outer nitroxyl line widths used in the simulations are 80 G. The experimental line widths must be at least this broad or the outer lines would be observable. Since V and VII have such similar sizes and shapes, the tumbling of the two molecules and the contributions to the line broadening due to slow tumbling would be expected to be similar. Since the nitroxyl inner and outer lines for V in low-viscosity solvents at room temperature range between 6 and 10 G, it is unlikely that the broadening of the nitroxyl lines in VII is due to slow tumbling. As noted above, the outer lines in the EPR spectra of VI at elevated temperature were difficult to detect because the outer line widths were substantially broader at higher temperatures than at room temperature. This was attributed to an increased uncertainty in J due to an increase in molecular motion. For VII, even at room temperature, the broadening of the outer lines suggests considerable uncertainty in the value of J.

The broad lines in the EPR spectra of VII would obscure any changes due to formation of a water adduct. Thus the EPR spectra give no indication whether adduct formation occurs for VII. At 75 °C the value of J is reduced to about 10 ± 10 G (Figure 4b). The values of J for amide VII are much more temperature dependent than for amide V (Figure 2). The two compounds differ only in the size of the nitroxyl ring. The large temperature dependence of J and the broad lines for VII, which contains a five-membered nitroxyl ring, suggests that conversion between ring conformations or amide–ring bond conformations which permit different extents of metal–nitroxyl-exchange interaction is a facile process. The temperature dependence of J and the narrow line widths for V, which contains a six-membered nitroxyl ring, suggest that whatever conformational changes occur for the six-membered nitroxyl in this temperature range have little impact on the magnitude of the metal–nitroxyl-exchange interaction. It has previously been observed that for compounds which differ only in the size of the nitroxyl ring, metal–nitroxyl-exchange interaction for the five-membered nitroxyl ring is sometimes smaller and sometimes larger than for the analogous compound containing a six-membered nitroxyl ring.[1,11,12] The present results suggest that the five-membered nitroxyl ring can adopt conformations which differ only slightly in overall energy but which differ greatly in the extent of exchange interaction between the nitroxyl group and a group attached to the nitroxyl ring. Therefore the differences observed previously between five- and six-membered nitroxyl rings may reflect which conformation of the five-membered nitroxyl is favored for a particular molecule.

Comparison with Prior Results. Prior papers in this series have demonstrated that the high-resolution spin–spin splitting patterns observed in room-temperature dilute-solution EPR spectra of metal–nitroxyl complexes are predominantly due to exchange interactions. The computer program CUNO used to fit the spectra in this study assumes exchange interactions. In order to estimate the relative exchange and dipolar contributions in other interacting spin systems, it is important to determine the dependence of the exchange interaction on the nature and conformations of the chemical bond pathway between the metal and the nitroxyl. Since exchange is a measure of orbital overlap, these studies also probe subtle features of the highest occupied and lowest unoccupied orbitals in fairly complex molecules.

We have previously reported that when the nitroxyl ring was attached to the porphyrin pyrrole position via an acrylic acid group the electron–electron interaction was greater for the trans isomer than for the cis isomer which correlates with greater π conjugation through the trans isomer than through the cis isomer.[11] In a series of spin-labeled vanadyl, copper, and silver porphyrins, the electron–electron interaction increased in the order $VO^{2+} < Cu^{2+} < Ag^{2+}$, which correlates with increasing delocalization of the unpaired electron into the porphyrin orbitals as monitored by EPR and ENDOR.[13] The results reported here for the spin-labeled copper porphyrins V and VI indicate that J correlates with the extent of porphyrin side chain conjugation. Thus the evidence obtained to date

(12) Boymel, P. M.; Braden, G. A.; Eaton, G. R.; Eaton, S. S. *Inorg. Chem.* **1980**, *19*, 735–739.
(13) More, K. M.; Eaton, S. S.; Eaton, G. R. *J. Am. Chem. Soc.* **1981**, *103*, 1087–1090.

indicates that the magnitude of J correlates with the extent of metal electron delocalization.

In systems of this complexity, one-parameter fits are not to be expected and many additional complexes will have to be examined before a quantitative description of exchange interactions emerges.

Acknowledgment. This work was supported in part by NIH Grant GM 21156. The Q-band spectrometer was purchased with partial support from NSF Grant CHE 78-16195. The assistance of K. T. Trevor and J. M. Neri in the preparation of the starting porphyrin (IV) is gratefully acknowledged.[3] Discussions with Professor J. M. Hornback contributed to some of the syntheses. Elemental analyses were performed by Spang Microanalytical Laboratory. B.M.S. thanks Shivaji University for a study leave.

Registry No. I, 64020-57-1; II, 78249-04-4; III, 78249-05-5; IV, 42953-54-8; V, 64012-89-1; VI, 64012-92-6; VII, 78248-88-1; 4-amino-2,2,6,6-tetramethylpiperidinyl-1-oxy, 14691-88-4; 4-hydroxy-2,2,6,6-tetramethylpiperidinyl-1-oxy, 2226-96-2; 3-amino-2,2,5,5-tetramethylpyrrolidinyl-1-oxy, 34272-83-8.

Contribution from the Departments of Chemistry, University of Denver, Denver, Colorado 80208, and University of Colorado at Denver, Denver, Colorado 80202

Metal–Nitroxyl Interactions. 22. Copper–Nitroxyl Spin–Spin Interaction as a Probe of Weak Orbital Overlaps in Derivatives of Copper Tetraphenylporphyrin

KUNDALIKA M. MORE, BHIMRAO M. SAWANT, GARETH R. EATON,* and SANDRA S. EATON

Received December 16, 1980

Derivatives of copper tetraphenylporphyrin have been prepared with nitroxyl groups attached via amide, ester, ether, or urea linkages to the ortho, meta, or para position of one phenyl ring. The magnitude of the copper–nitroxyl spin–spin coupling constant, J, was determined from the EPR spectra in low-viscosity solvents at room temperature. When the position of the phenyl ring substituent is varied, J decreases in the order ortho substituted $\gg$ para substituted $\geq$ meta substituted. The larger value of J for a substituent at the para position than at the meta position suggests that the spin–spin interaction occurs via the π orbitals of the phenyl ring. The much larger values of J for substituents at the ortho position than at the meta or para positions suggest an additional pathway for spin–spin interaction. The proximity of the ortho substituents to the porphyrin ring may result in overlap of orbitals on the substituents with the porphyrin π orbitals. In some of the complexes, there may also be a weak interaction between keto groups on the ortho substituents and the copper atom.

Introduction

We have recently reported the observation of high-resolution electron spin–electron spin splitting in the EPR spectra of spin-labeled copper(II) and silver(II) complexes in solution at room temperature.[1-5] Under these conditions the splittings are due to electron–electron-exchange interactions. The magnitude of the spin–spin coupling constant, J, was found to be sensitive to details of the molecular stereochemistry and electron delocalization.[4,5] Values of J between $\sim$2 and $\sim$3000 G ($\sim 2 \times 10^{-4}$ to $\sim$0.3 cm^{-1}) can be determined from the EPR spectra of spin-labeled copper complexes.[1] Thus interactions which are too weak to be readily probed by other techniques can readily be studied in spin-labeled metal complexes.

Several studies by other groups (see below) have found that unpaired spin density is larger at the ortho positions of the phenyl rings in paramagnetic metallotetraphenylporphyrins than at the meta and para positions. These results have led to proposals of specific orbital interactions between the ortho substituents and the porphyrin π system. In order to use metal–nitroxyl interactions to probe the spin-delocalization into the phenyl ring and to examine possible mechanisms for interaction of ortho substituents with the porphyrin ring, we have prepared a series of phenyl-substituted derivatives of copper tetraphenyl porphyrin which are spin-labeled at the ortho, meta, or para position of one phenyl ring, I–XII. This series permits comparison of amide linkages at the ortho, meta, and para positions, and a comparison of three amide, two ester, an ether, and a urea linkage at the ortho position. EPR spectra were taken in the presence and absence of coordinating solvents and as a function of temperature to provide information concerning the mechanism of spin–spin interaction.

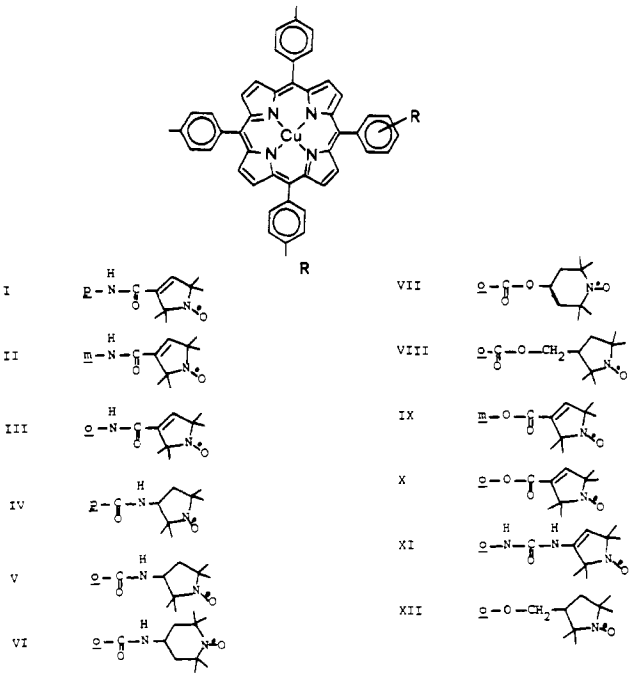

Experimental Section

Physical Measurements. All spectra were obtained in dried purified solvents. Infrared spectra were obtained in Nujol mulls on a Perkin-Elmer 337 grating spectrometer. Visible spectra were obtained

* To whom correspondence should be addressed at the University of Denver.

(1) Eaton, S. S.; Eaton, G. R. *Coord. Chem. Rev.* **1978**, *26*, 207–262.
(2) Boymel, P. M.; Eaton, G. R.; Eaton, S. S. *Inorg. Chem.* **1980**, *19*, 727–735.
(3) Boymel, P. M.; Braden, G. A.; Eaton, G. R.; Eaton, S. S. *Inorg. Chem.* **1980**, *19*, 735–739.
(4) More, K. M.; Eaton, S. S.; Eaton, G. R. *J. Am. Chem. Soc.* **1981**, *103*, 1087–1090.
(5) More, K. M.; Eaton, S. S.; Eaton, G. R. *Inorg. Chem.*, in press.

0020-1669/81/1320-3354$01.25/0